LUND UNIVERSITY

Spectroscopic identification of ethanol-water conformers by large-amplitude hydrogen bond librational modes.

Andersen, J; Heimdal, Jimmy; Wugt Larsen, R

Link to publication

Spectroscopic identification of ethanol-water conformers by large-amplitude hydrogen bond librational modes

J. Andersen, J. Heimdal, and R. Wugt Larsen

Spectroscopic identification of ethanol-water conformers by large-amplitude hydrogen bond librational modes

J. Andersen,[1] J. Heimdal,[2] and R. Wugt Larsen[1,a]

[1]*Department of Chemistry, Technical University of Denmark, Kemitorvet 206, 2800 Kongens Lyngby, Denmark*
[2]*MAX-IV Laboratory, Lund University, P.O. Box 118, 22100 Lund, Sweden*

The far-infrared absorption spectra have been recorded for hydrogen-bonded complexes of water with ethanol embedded in cryogenic neon matrices at 2.8 K. The partial isotopic H/D-substitution of the ethanol subunit enabled by a dual inlet deposition procedure enables the observation and unambiguous assignment of the intermolecular high-frequency out-of-plane and the low-frequency in-plane donor OH librational modes for two different conformations of the mixed binary ethanol/water complex. The resolved donor OH librational bands confirm directly previous experimental evidence that ethanol acts as the $O \cdots HO$ hydrogen bond acceptor in the two most stable conformations. In the most stable conformation, the water subunit forces the ethanol molecule into its less stable *gauche* configuration upon dimerization owing to a cooperative secondary weak $O \cdots HC$ hydrogen bond interaction evidenced by a significantly blue-shift of the low-frequency in-plane donor OH librational band origin. The strong correlation between the low-frequency in-plane donor OH librational motion and the secondary intermolecular $O \cdots HC$ hydrogen bond is demonstrated by electronic structure calculations. The experimental findings are further supported by CCSD(T)-F12/aug-cc-pVQZ calculations of the conformational energy differences together with second-order vibrational perturbation theory calculations of the large-amplitude donor OH librational band origins. © *2015 AIP Publishing LLC.* [http://dx.doi.org/10.1063/1.4937482]

I. INTRODUCTION

A long-standing challenge for the physical sciences is to accurately describe how remarkable macroscopic properties of condensed phases, biological systems, and materials emerge from the interplay between the different classes of non-covalent intermolecular interactions such as directional hydrogen bonding, long-range London dispersion interactions, and short-range steric repulsion between molecules. These different classes of non-covalent interactions are both responsible for the thermodynamic anomalies associated with bulk liquid mixtures, the three-dimensional folding dynamics for biological macromolecules, and the mechanical properties of many functional materials.

In the context of biological systems, the interplay between multiple intermolecular organic hydrogen bond interactions ranging from weak $O \cdots HC$ and $\pi \cdots HO$ (<5–20 kJ mol^{-1}) to stronger classical $O \cdots HO$ (~20–60 kJ mol^{-1}) hydrogen bonds often governs the functionality of many biological macromolecules as these directional intermolecular interactions are able to control the formation of specific enzyme-substrate complexes. For this reason, mixed hydrogen-bonded molecular complexes involving the simplest flexible alcohols are particular interesting model systems since both strong intermolecular $O \cdots HO$ hydrogen bonds and weak secondary intermolecular $O \cdots HC$ hydrogen bond interactions are

realized simultaneously. The binary mixed complex of the simplest flexible alcohol, ethanol, with water can be regarded as a prototypical target system which is still amenable to high levels of theoretical *ab initio* methodologies. This 1:1 ethanol/water complex has turned out to represent one of the simplest mixed hydrogen-bonded molecular complexes of a flexible subunit where the intermolecular hydrogen bond formation affects the internal conformational degrees of freedom. The isolated ethanol molecule exists both in a *trans* (denoted *t*) and in two enantiomeric *gauche* configurations (denoted g^+ and g^-) being ≈0.5 kJ mol^{-1} higher in electronic energy.[1–4] Upon complexation with water, several studies have suggested that the ethanol molecule is forced into the less stable *gauche* configuration.

A sensitive and well-established spectroscopic probe for hydrogen-bonded molecular complexes is the vibrational OH-stretching manifold of the donor subunits[5,6] and a recent combined infrared and Raman investigation has monitored the donor OH-stretching spectral red-shifts for mixed 1:1 complexes of water with methanol and ethanol adiabatically cooled in supersonic jet expansions.[7,8] The vibrational assignments confirmed microwave molecular beam studies[9] that water acts as the hydrogen bond donor in the most stable conformations of both mixed alcohol/water complexes.[7] Based on the lower limit of the effective conformational temperature in the supersonic jet expansions of 10 K, the energy difference between the two most stable conformations of the mixed ethanol/water complex has been estimated to be higher than 0.2 kJ mol^{-1} from dedicated collisional relaxation

---
a)Author to whom correspondence should be addressed. Electronic mail: rewl@kemi.dtu.dk

experiments.[8] However, a recent microwave molecular beam work[9] has only identified the single conformation with ethanol as the hydrogen bond acceptor in the g^+ configuration and more experimental evidence has been welcomed to shed more light on this internal conformational isomerism issue.

In a recent work, it was demonstrated how the strength, directionality, and anharmonicity of mixed alcohol/water complexes can be probed more *directly* via the large-amplitude intermolecular donor OH librational modes. These direct spectroscopic observables detected in the challenging far-infrared spectral region between 300 and 600 cm^{-1} have been shown to enable an accurate characterization of the intermolecular potential energy landscape between the hydrogen bond partners.[10–13] Its nature as a localized motion of the donor hydrogen atom makes the high-frequency out-of-plane donor OH librational mode an excellent probe for the intermolecular hydrogen bond interaction in a similar fashion as the Badger-Bauer relationship associated with the bathochromic shift of the intramolecular donor vibrational OH-stretching mode.[14] A stronger intermolecular hydrogen bond results in a more hindered internal rotational motion and an increase of the band origin for this high-frequency hydrogen bond donor mode. In the mixed complexes of water with aliphatic alcohols, these donor OH librational spectral signatures thus act as a measure of the hydrogen bond acceptor strength of the alcohol molecule. In the present work, we demonstrate how the low-frequency in-plane donor OH librational mode of mixed ethanol/water complexes, essentially a hindered overall c-axis rotation of the water subunit, provides an excellent probe for the cooperative secondary O $\cdots$ HC hydrogen bond interactions, which allows for a rigorous benchmarking of theory.

II. EXPERIMENTAL

A pre-cooled (77 K) gas flow of neon (L'Air Liquide, 99.999%) was deposited with a flow rate of 0.02 mol/h on a gold-plated oxygen-free high thermal conductivity (OFHC) copper mirror at 3.6 K inside an immersion helium cryostat (IHC-3) modified for matrix isolation spectroscopy.[13,15] The pre-cooling of neon significantly reduces the heat load on the copper mirror and enables a total deposition time of 1–2 h per experiment. The pre-cooled neon gas flow was subsequently doped with "freeze-pump-thaw" purified C_2H_5OH (Sigma Aldrich, 99.9%), and H_2O (Milli-Q) samples and isotopically substituted C_2H_5OH-d1 (Sigma Aldrich, 99.0% D), C_2H_5OH-d6 (Sigma Aldrich, 99.0% D) and D_2O (Sigma Aldrich, 99.5% D) samples via separate inlet tubes with mixing ratios of ≃0.5–5 permille. The combination of resistive heaters and feedback electronics was employed to maintain a stable mirror temperature at 2.8 ± 0.1 K before and after the neon matrix depositions. The cold head was mounted with interchangeable CsI and polymethylpentene (TPX) windows and combined IR and THz single-beam sample spectra were collected by a Bruker IFS 120 FTIR spectrometer employing tungsten and globar lamps as the radiation sources. Liquid nitrogen cooled HgCdTe (broadband) and InSb detectors combined with Ge/KBr and CaF$_2$ beam splitters, respectively, were

employed for the spectral region above 600 cm^{-1}. A Si-bolometer operating at 4.2 K combined with a 6 μm multilayer Mylar beam splitter was employed for the 30–650 cm^{-1} spectral region. In all experiments, the doped neon matrices were annealed up to 9 K for the study of temperature effects. Single-beam background spectra were subsequently collected of the evacuated cryostat. A spectral resolution in the range from 0.1 to 1.0 cm^{-1} was selected depending on the observed band widths.

III. VIBRATIONAL ASSIGNMENTS FOR THE MIXED ETHANOL/WATER COMPLEX

Figs. 1 and 2 show selected spectral regions from a series of far-infrared absorption spectra (200–600 cm^{-1}) collected for several millimeter thick cryogenic neon matrices doped with pure water (H_2O:Ne) = (1:1700), pure ethanol (C_2H_5OH:Ne) = (1:1200), and different isotopically substituted ethanol/water mixtures (C_2H_5OH:H_2O:Ne) = (2:1:1700) at 2.8 K. In previous far-infrared matrix isolation studies of water embedded in neon, the pure complexes of water have been explored extensively.[13,16–19] In the spectral region above 300 cm^{-1}, the strong intermolecular high-frequency out-of-plane and low-frequency in-plane donor OH librational bands of the water dimer embedded in neon matrices have previously been assigned at 522.4 cm^{-1} and 309.1 cm^{-1} (Fig. 1), respectively.[16] The low-frequency donor in-plane OH librational band is slightly overlapped with the c-axis librational band of cyclic water trimer previously assigned at 310.8 cm^{-1}. In addition, a number of five combination bands have previously been observed for the cyclic water trimer where the strongest transitions have been assigned at 280.0, 386.8 and 414.1 cm^{-1}.[17]

The absorption spectrum of ethanol below 300 cm^{-1} has been widely studied by both experiment and theory owing to the *trans-gauche* isomerism and the proximity
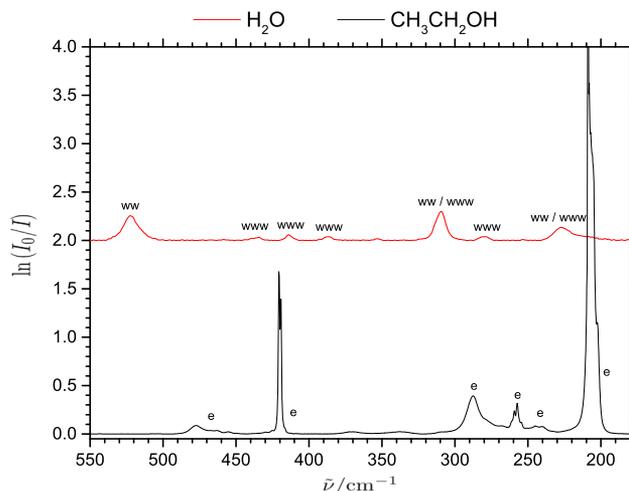

FIG. 1. The observed far-infrared absorption spectra (200-550 cm^{-1}) of pure water and pure ethanol embedded in neon matrices at 2.8 K. The vibrational assignments for the ethanol monomer is denoted e and the vibrational assignments for the water complexes are denoted ww (dimer) and www (trimer), respectively.
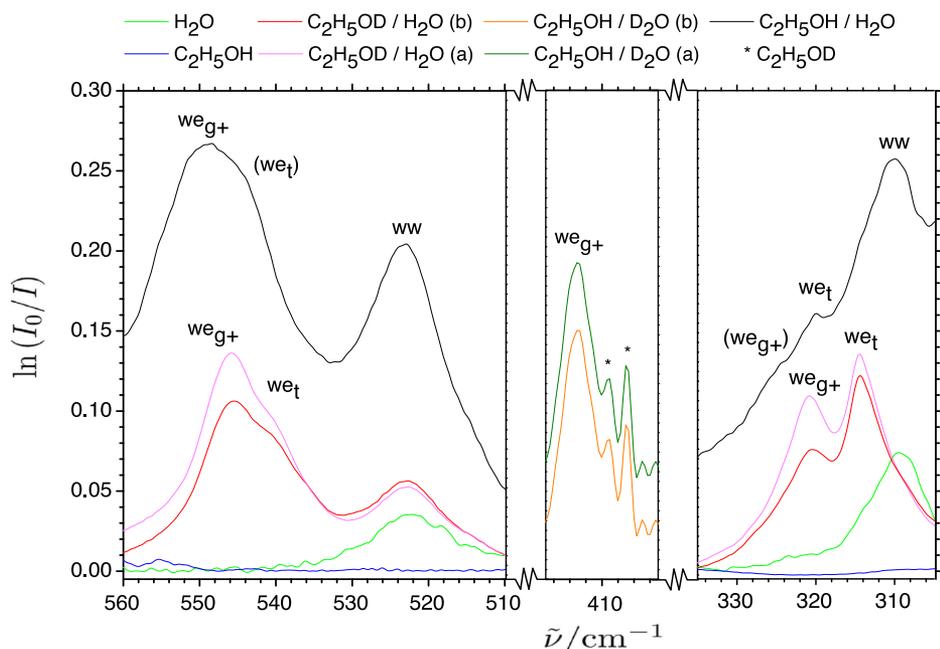
FIG. 2. The observed far-infrared absorption spectra of pure water, pure ethanol, and different isotopic ethanol/water mixtures embedded in neon matrices at 2.8 K before annealing (b) and after annealing (a) to 9 K in the spectral regions belonging to the out-of-plane OH (left), out-of-plane OD (center), and in-plane OH (right) donor librational modes. The proposed vibrational assignments for the mixed isotopic complexes of water (w) and ethanol (e) in the *trans* and *gauche+* conformations are denoted we_t and we_{g+}, respectively (see text), whereas the vibrational assignments for the water dimer is denoted as ww. The asterisks denote traces of ethanol-d1 impurities.

and the large vibrational amplitudes for the OH and CH$_3$ torsional motion of this molecule.[1,2,20–24] A previous work has addressed the complex asymmetric top-asymmetric frame internal rotation spectrum of the flexible ethanol monomer and cites the numerous previous microwave investigations employed to characterize the vibrational ground state and the conformational *trans-gauche* isomerism of ethanol.[22] We also refer to this comprehensive work for further details about the excited energy sub-levels of ethanol associated with the large-amplitude OH and CH$_3$ torsional degrees of freedom which has been complemented by far-infrared gas-phase absorption spectroscopy[1,21] and more recently by Raman jet spectroscopy.[23] The gas-phase absorption study assigned a single band observed at 202.6 cm^{-1} to the fundamental OH torsional transition of the *trans* conformation and two other bands observed at 195.8 and 243.1 cm^{-1} to the *gauche* conformation ($g^+ \leftarrow g^-$ and $g^- \leftarrow g^+$ transitions, respectively). The Raman jet study assigned two other bands observed at 199.1 cm^{-1} ($g^+ \leftarrow g^+$) and 240 cm^{-1} ($g^- \leftarrow g^-$).[23] The far-infrared absorption spectrum of ethanol embedded in cryogenic argon matrices has previously just revealed two strong transitions observed at 211 and 264 cm^{-1} besides the strong CCO bending fundamental transition at 416.5 cm^{-1}.[20] In the present far-infrared spectra of ethanol embedded in more inert cryogenic neon matrices, a series of weak, medium-intensity, and strong bands are observed besides the strong CCO bending fundamental transition at 419.9 cm^{-1} (Fig. 1). A strong sharp transition appears at 208.9 cm^{-1} with two less intense shoulders observed at 206.5 cm^{-1} and 202.4 cm^{-1}. The spectra further reveal a broad medium-intense band at 287.4 cm^{-1}, a medium-intense band structure around 258 cm^{-1}, and a weaker band structure around 243 cm^{-1}. These observed spectral features are in qualitative agreement with the coupled OH and CH$_3$ torsional sub-bands predicted previously from a two-dimensional *ab initio* Hamiltonian.[24] A more detailed interpretation of the observed spectral features is beyond the scope of the present

work concerned with the donor OH librational modes of the mixed ethanol/water complex. Both the partial and complete H/D substitution of ethanol red-shifts the disturbing torsional sub-band component at 287.4 cm^{-1} to below 200 cm^{-1} and thereby paves the way for the spectral region between 300 and 600 cm^{-1}.

The far-infrared spectra recorded for neon matrices doped with regular ethanol and regular water simultaneously at moderate concentrations reveal new distinct bands in the close vicinity to the high-frequency out-of-plane and low-frequency in-plane donor OH librational bands of water dimer. A weak band seems to emerge around 320 cm^{-1} on the shoulder of the in-plane donor OH librational band of water dimer at 309.1 cm^{-1} (Fig. 2, right inset). This spectral region is still affected by the broad torsional sub-band component of ethanol observed in the neon matrices at 287.4 cm^{-1}. In addition, a stronger and more distinct but somewhat broader band clearly emerges in the spectrum at 551.6 cm^{-1} for neon matrices doped with ethanol and water (Fig. 2, left inset). Both observed bands and in particular the latter band at 551.6 cm^{-1} are thus blue-shifted relative to the established donor OH librational transitions of the water dimer (Table I). This observation supports the trend from the previous investigation of mixed binary complexes of water with methanol and *t*-butanol embedded in cryogenic neon matrices.[25] This previous work has established that water acts as the hydrogen bond donor in the most stable binary mixed complexes with methanol and *t*-butanol. This hydrogen bond donor/acceptor relationship gives rise to similar out-of-plane and in-plane donor OH librational motions for the mixed alcohol/water complexes as observed for the donor subunit in the water dimer. The animated donor OH librational normal mode pictures are shown for the mixed ethanol/water complex in Fig. 3. The high-frequency out-of-plane donor OH libration can be described as a localized motion of the "bound" hydrogen atom. This localized mode turns out to be an excellent probe for the intermolecular hydrogen bond

TABLE I. The observed high-frequency out-of-plane and low-frequency in-plane donor OH (OD) librational band origins (cm^{-1}) for the water dimer and the two most stable isotopic complexes of water (w) and ethanol (e) in the *trans* (denoted we_t) and *gauche+* (denoted we_{g+}) conformations embedded in neon matrices at 2.8 K.

Donor-acceptor	$\nu_{lib, out-of-plane}$	$\nu_{lib, in-plane}$	Donor-acceptor	$\nu_{lib, out-of-plane}$	$\nu_{lib, in-plane}$
ww	522.4[a]	309.1[a]	$w(d2)w(d2)$	393.2[a]	233.5[a]
we_{g+}	551.6	324.7	$w(d2)e_{g+}$	412.5	239.6
we_t	(545.4)[b]	(320.4)[b]	$w(d2)e_t$	c	c
$we_{g+}(d1)$	545.6	320.9	$w(d2)e_{g+}(d1)$	d	238.2
$we_t(d1)$	541.1	314.7	$w(d2)e_t(d1)$	c	c
$we_{g+}(d6)$	545.6	320.9			
$we_t(d6)$	540.1	313.9			

[a]Ceponkus *et al.*[13]
[b]Tentative assignments due to strong overlaps with we_{g+}.
[c]Not observed.
[d]Overlap with the CCO bending mode of ethanol-d1.

interaction[10,11,25] in the same way as the pronounced red-shift of the intramolecular donor OH-stretching mode. The observed high-frequency out-of-plane OH librational band origin of 551.6 cm^{-1} thus indicates a significantly stronger intermolecular hydrogen bond for the mixed ethanol/water complex than the corresponding mixed methanol/water complex having a band origin of 527.5 cm^{-1} but a slightly weaker hydrogen bond than for the mixed *t*-butanol/water complex having a band origin of 556.6 cm^{-1}.[25] These preliminary and entirely spectroscopic interpretations about the relative hydrogen bond energies shall be supported with predictions from exploratory quantum chemical calculations in the theoretical section. A few other experimental studies for mixed water complexes with methanol and ethanol embedded in cryogenic matrices of nitrogen and argon have been reported in Refs. 26 and 27. In the most perturbing matrix environment of nitrogen, a reversed hydrogen bond donor/acceptor relationship for the alcohol/water complexes has been observed although severe site effects blurred the observed spectral signatures. This has been explained by weak cooperative attractive interactions between the OH groups and the N$_2$ host molecules.[28] In the mixed complexes where the alcohol molecule acts as the hydrogen bond donor, both dangling OH groups of the water acceptor subunit might interact with N$_2$ host molecules and thereby increasing the acceptor character of the O nuclei on the water molecule. This

effect might strengthen the intermolecular interaction to the alcohol subunit and overcome the energy barrier between the different alcohol-water conformers.[28]

The dual inlet deposition procedure designed for partial isotopic H/D substitutions of the individual subunits enables the unambiguous identification of the proposed hydrogen bond donor/acceptor roles in the cryogenic neon environment. The H/D substitution on the water subunit introduces a significant red-shift from 551.6 cm^{-1} to 412.5 cm^{-1} which further confirms that water acts as hydrogen bond donor (Fig. 2, central inset). The observed OH/OD band origin ratio of 1.34 is rather close to the theoretical value of $\sqrt{2}$ expected for a localized harmonic hydrogen motion and supports an assignment to the out-of-plane donor OD librational mode for the complex of D$_2$O with ethanol. This band origin is slightly larger than the corresponding donor OD librational band origin assigned previously at 397.6 cm^{-1} for the less stable mixed complex of methanol with D$_2$O embedded in neon.[25] The low-frequency in-plane donor OD librational mode is shifted into the congested spectral region belonging to the coupled OH and methyl torsional modes of ethanol making the assignment of this band difficult although a tentative assignment can be proposed at 239.6 cm^{-1} (not shown). A similar partial H/D substitution on ethanol deposited with regular water introduces solely a small red-shift of 6 cm^{-1} for the high-frequency donor OH librational band supporting the proposed hydrogen bond acceptor role of the ethanol subunit (Fig. 2, left inset). The far-infrared spectra for ethanol-d1/water mixtures doped in neon, however, all seem to contain two distinct bands at 545.6 cm^{-1} and 541.1 cm^{-1} in this spectral region. These observations are supported by subsequent annealing experiments where the mirror temperature is raised to 9 K to allow the guest molecules to diffuse within the soft neon matrices. The annealing in particular favors the diffusion of the smaller water molecules in the soft neon matrices and the excess of ethanol should thereby trigger the formation of mixed ethanol/water complexes. The post-annealing spectrum recorded after subsequent cooling to 3 K reveals a significant increase of both band intensities whereas the high-frequency out-of-plane donor OH librational band of water dimer at 522.9 cm^{-1} is almost unaffected by annealing (Fig. 2, left inset). The post-annealing intensity of the band observed at 545.6 cm^{-1} is significantly larger than the post-annealing intensity of the other band observed at
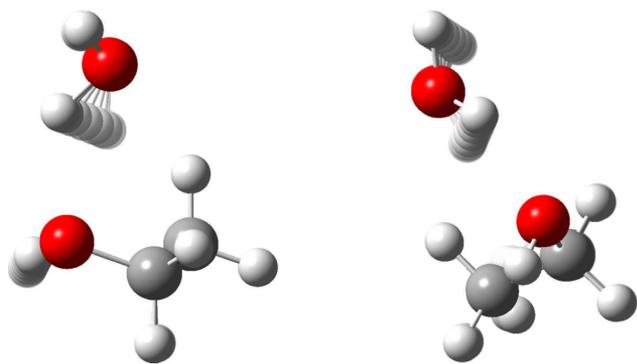

FIG. 3. Normal mode pictures of the large-amplitude high-frequency out-of-plane (left) and low-frequency in-plane (right) donor OH librational modes of the most stable conformation of the mixed hydrogen-bonded ethanol/water complex (see text).

541.1 cm^{-1}. This observation suggests that these overlapped bands originate from two conformations of the mixed ethanol-d1/water complex with the band at 545.6 cm^{-1} assigned to the most stable conformation. The partial H/D substitution on the ethanol sample turns out to have an even more pronounced effect on the low-frequency in-plane donor OH librational signature where two completely separated bands are observed at 320.9 cm^{-1} and 314.7 cm^{-1}, respectively (Fig. 2, right inset). The post-annealing spectra again reveal a changed relative intensity compared to the pre-annealing spectra. The more significant post-annealing intensity increase of the band observed at 320.9 cm^{-1} suggests an assignment to the most stable conformation of the mixed ethanol-d1/water complex. In the same fashion, the complete H/D substitution on the ethanol sample enables the identification of two conformations of the mixed ethanol-d6/water complex with band origins red-shifted by less than 1 cm^{-1} relative to the ethanol-d1/water conformations (see Table I). In order to shed further light on the proposed assignments and clarify the observation of two conformations of the ethanol-d1/water and ethanol-d6/water complexes, we consult exploratory electronic structure calculations.

IV. EXPLORATORY QUANTUM CHEMICAL CALCULATIONS

The quantum chemical software packages Gaussian09 (Rev. D.01)[29] and Turbomole (ver. 6.6)[30,31] have both been employed for *ab initio* molecular orbital and supplementary density functional theory (DFT) calculations. The equilibrium geometries of the water and ethanol subunits and the different conformations of the mixed ethanol-water complexes were all optimized and the corresponding electronic energies calculated employing the canonical B3LYP level,[32] the dispersion-corrected B3LYP-D3 approach,[33] and the second order Möller-Plesset (MP2) methodology[34,35] coupled with Dunning's augmented correlation-consistent triple-zeta (aug-cc-pVTZ) and quadruple-zeta (aug-cc-pVQZ) basis sets.[36] The root-mean-square force criterion has been set to 10^{-6} (atomic units) for all the equilibrium geometry optimizations. The electronic energies for these optimized equilibrium geometries were subsequently calculated employing both the canonical and the explicitly correlated coupled-cluster approaches with single and double with perturbative triple excitations, CCSD(T)[37] and CCSD(T)-F12,[38] in order to optimize the extent of electron correlation in combination with the same Dunning basis sets. The basis set superposition errors[39] have been accounted for by the counterpoise method of Boys and Bernardi.[40] The harmonic vibrational frequencies and overall vibrational zero-point energy (ZPE) contributions for the monomers and ethanol-water conformations have been calculated employing the doubly harmonic approximation whereas the anharmonic frequencies have been calculated using the VPT2 approach[41] as implemented in Gaussian09 (Rev. D.01).[29] In a series of calculations, the secondary CH···O hydrogen bond contact between the terminal CH group on the ethanol subunit and the lone pair of the water subunit was kept fixed (Keyword = ModRedundant) in the

geometry optimization in order to investigate the dependence of the donor OH-stretching and donor OH librational frequencies on this intermolecular CH···O contact strength.

V. DISCUSSION

A. Hydrogen-bonded conformations of the mixed ethanol/water complex

In line with previous theoretical predictions of the intermolecular potential energy landscape for the binary ethanol/water complex,[7,9] five distinguishable conformations have been investigated. Fig. 4 illustrates the relative electronic binding energy D_0 calculated with the CCSD(T)-F12/aug-cc-pVQZ approach for these five most stable conformations optimized at the MP2/aug-cc-pVQZ level of theory. The changes of the harmonic vibrational zero-point energy upon complexation (ΔZPE) have been calculated at the MP2/aug-cc-pVTZ level of theory. This combined methodology is regarded as the benchmark level of theory as illustrated by the series of predictions of the electronic binding energy D_e for the most stable mixed complex of water with ethanol listed in Table II. The listed predictions provide the results from combined quantum chemical methodologies employed for the geometry optimizations and subsequent single-point electronic energy calculations. These computations show that the canonical B3LYP functional[32] underestimates the binding
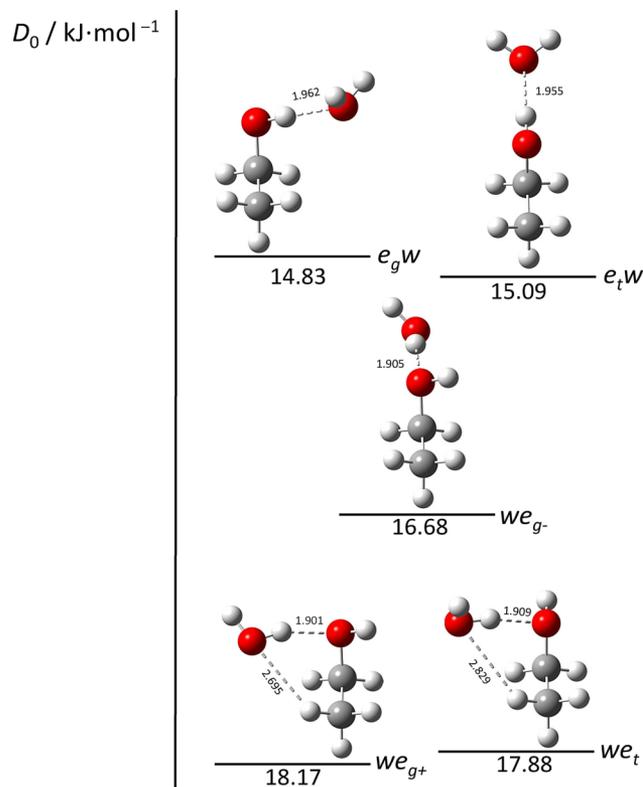
FIG. 4. The intermolecular potential energy landscape including the most stable conformations of the mixed 1:1 complex of ethanol and water in terms of the electronic binding energies D_0 calculated employing the CCSD(T)-F12/aug-cc-pVQZ approach for the five most stable conformations optimized at the MP2/aug-cc-pVQZ level of theory (see text).

TABLE II. The electronic dissociation energy D_e of the two most stable conformations of the ethanol/water complex (denoted we_{g+} and we_t) and the difference of electronic dissociation energy between the conformations $\Delta E_e = D_e(we_{g+}) - D_e(we_t)$ predicted from combined quantum chemical methodologies for the geometry optimization and electronic energy calculations employing Dunning's augmented correlation-consistent triple zeta (aug-cc-pVTZ) and quadruple zeta (aug-cc-pVQZ) basis sets.

Optimization[a]	Electronic energy	$D_e(we_{g+})$/kJ mol^{-1}	ΔE_e/kJ mol^{-1}
B3LYP/aug-cc-pVTZ	B3LYP/aug-cc-pVTZ	20.99	0.03
B3LYP-CP/aug-cc-pVTZ[b]	B3LYP/aug-cc-pVTZ	20.69	0.04
B3LYP-CP/aug-cc-pVTZ[b]	CCSD(T)/aug-cc-pVTZ	26.33	0.03
B3LYP-D3/aug-cc-pVTZ	B3LYP-D3/aug-cc-pVTZ	28.02	0.61
B3LYP-D3-CP/aug-cc-pVTZ[b]	B3LYP-D3/aug-cc-pVTZ	27.68	0.62
B3LYP-D3-CP/aug-cc-pVTZ[b]	CCSD(T)/aug-cc-pVTZ	27.96	0.48
MP2/aug-cc-pVTZ	MP2/aug-cc-pVTZ	27.27	0.36
MP2-CP/aug-cc-pVTZ[b]	MP2/aug-cc-pVTZ	24.52	0.37
MP2-CP/aug-cc-pVTZ[b]	CCSD(T)/aug-cc-pVTZ	27.46	0.54
MP2-CP/aug-cc-pVTZ[b]	CCSD(T)-F12/aug-cc-pVTZ	27.01	0.58
MP2/aug-cc-pVQZ	MP2/aug-cc-pVQZ	26.61	0.41
MP2-CP/aug-cc-pVQZ[b]	MP2/aug-cc-pVQZ	25.24	0.40
MP2-CP/aug-cc-pVQZ[b]	CCSD(T)/aug-cc-pVQZ	26.63	0.58
MP2-CP/aug-cc-pVQZ[b]	CCSD(T)-F12/aug-cc-pVQZ	26.50	0.56

[a]RMS force criterion set to 10^{-6} (atomic units) for all geometry optimizations.

[b]CP = Counterpoise Correction applied.

energy D_e for the most stable mixed complex of water with ethanol by ca. 20% (5.5 kJ mol^{-1}) whereas the B3LYP-D3 approach including Grimme and co-worker's dispersion corrections[33] slightly overestimates this binding energy by ca. 5% (1.5 kJ mol^{-1}) relative to the benchmark D_e-value of 26.5 kJ mol^{-1}. This predicted electronic binding energy is significantly larger than the predicted binding energy for the mixed methanol/water complex but slightly smaller than the predicted binding energy for the t-butanol/water complex as expected.[25] The harmonic ΔZPE-correction of 8.3 kJ mol^{-1} then translates this value into an absolute electronic binding energy D_0 of 18.2 kJ mol^{-1} for the most stable conformation of the ethanol/water complex as shown in Fig. 2.

In the three most stable conformations, the water subunit acts as the hydrogen bond donor. These three structures are denoted as *we* whereas the remaining two structures having ethanol as the hydrogen bond donor are denoted as *ew*. In the three most stable forms having water as the hydrogen bond donor, not only the conformation (*trans* or *gauche*) of the ethanol subunit is relevant but also the choice of the acceptor lone pair on ethanol. In the *gauche*+ conformation, the O–H bond is rotated clockwise by 120° relative to the *trans* conformation in the perspective along the O–C bond employing a Newman projection. In the conformations of the mixed complex of ethanol with water as the hydrogen bond donor, a new asymmetric center emerges at the oxygen atom of the alcohol subunit due to the two potential acceptor oxygen lone pairs and two potential enantiomeric conformations. Looking again along the O–C bond vector, the lone pair in a clockwise direction from the OH bond is denoted by the right lone pair as shown in Fig. 4 in line with previous works.[7,9] In the case of two non-distinguishable enantiomeric conformations, we discuss the conformation where this right lone pair is engaged in the hydrogen bond. As illustrated in Fig. 4, the we_{g+} conformation with a hydrogen bond to

the right lone pair of ethanol is predicted to be the most stable and compact conformation of the mixed ethanol/water complex at the benchmark level. In contrast to the third most stable we_{g-} conformation, the we_{g+} conformation is further stabilized by a cooperative secondary hydrogen bond interaction between the terminal CH group on ethanol and the oxygen lone pair on the water subunit with a contact distance predicted to 2.695 Å at the MP2/aug-cc-pVQZ level (see Fig. 4), although this weaker secondary interaction bends the primary O$\cdots$HO hydrogen bond slightly from a linear arrangement. In the most stable conformation the water subunit thus forces the ethanol hydrogen bond partner into its less stable *gauche* conformation upon complexation although the *trans* conformation is the most stable for an isolated ethanol molecule. This is considered as one of the most elementary cases together with hydroxyacetone[42] of adaptive aggregation, where a non-rigid molecule is forced into a less stable conformation upon non-covalent binding to a hydrogen bond donor molecule to optimize the mutual interaction energy. The second most stable conformation of the mixed complex having water as the hydrogen bond donor and the acceptor ethanol subunit in its *trans* configuration is also further stabilized by a cooperative secondary O$\cdots$HC contact. However, this secondary interaction is less strong with a contact distance predicted to 2.829 Å at the MP2/aug-cc-pVQZ level (see Fig. 4). The small difference of electronic dissociation energy between these two most stable conformations $\Delta E_e = D_e(we_{g+}) - D_e(we_t)$ listed in Table II seems to depend on the computational methodology. The canonical B3LYP approach predicts almost identical electronic dissociation energies whereas the dispersion-corrected B3LYP-D3 approach slightly overestimates this difference in the electronic dissociation energy relative to the benchmark CCSD(T)-F12/aug-cc-pVQZ value of 0.56 kJ mol^{-1} for ΔE_e. The effect of the ZPE contributions and in particular the influence of the donor OH librational motion

on the electronic dissociation energy must be considered before reaching any further conclusions.

B. Vibrational zero-point energy contributions

The change of vibrational ZPE upon intermolecular hydrogen bond formation is notoriously complicated to predict by quantum chemical methods in particular for the large-amplitude and highly anharmonic intermolecular hydrogen bond librational motions. In a previous combined jet and neon matrix isolation far-infrared study of methanol dimer, the similar high-frequency out-of-plane donor OH librational band was observed and assigned at 560 cm^{-1}.[12] This study reported an overall sum of anharmonic contributions to this out-of-plane donor OH librational fundamental transition in the order of 100 cm^{-1} by employing vibrational second-order perturbation theory (VPT2).[41] In the combination with the benchmark harmonic band origin of 660 cm^{-1} predicted at the LCCSD(T)-F12 level, the anharmonic predicted band origin of 560 cm^{-1} turned out to be in excellent agreement with the experimental neon matrix findings. In a previous investigation of the mixed methanol/water complex, a similar anharmonic VPT2 analysis[41] at the MP2/aug-cc-pVTZ level also suggested anharmonicity contributions in the order of 15%-20% for the corresponding high-frequency out-of-plane donor OH librational transition.[25] In this previous work, standard vibrational frequency calculations at the MP2/aug-cc-pVTZ level provided harmonic band origins of 647 and 669 cm^{-1} for the high-frequency out-of-plane donor OH librational transitions for the mixed complexes of water with methanol and *t*-butanol, respectively.[25] The ordering of these harmonic values is in qualitative agreement with the previous experimental findings suggesting that similar harmonic predictions for the ethanol/water complex should fit into this picture. The harmonic calculations for the out-of-plane donor OH librational modes of the two most stable ethanol/water conformations at the MP2/aug-cc-pVTZ level indeed predict these band origins between 647 and 669 cm^{-1} as expected. However, the harmonic band origin for the most stable we_{g+} conformation is predicted at 654 cm^{-1} with the harmonic band origin for the less stable we_t conformation predicted at 660 cm^{-1} in contrast to our proposed experimental assignments based on evident annealing effects (see Table I). An anharmonic VPT2 analysis at the MP2/aug-cc-pVTZ level, however, reverses the order of predicted band origins (549 cm^{-1} for the we_{g+} conformation and 543 cm^{-1} for the we_t conformation) and confirms anharmonicity contributions of 15%-20%. A similar analysis of the low-frequency in-plane donor OH librational modes and the entire sets of large-amplitude intermolecular vibrational transitions for the non-rigid hydrogen-bonded ethanol/water complex would be to stretch the reliability of the VPT2 approach. Table III thus provides the harmonic vibrational ZPE contribution for mixed isotopic complexes of water with ethanol predicted at the feasible MP2/aug-cc-pVTZ level of theory.

The incorporation of the calculated vibrational ZPE contributions has a large impact as evidenced by the resulting absolute ground-state dissociation energies D_0 of the different we_t and we_{g+} conformations listed in Table III. The total

TABLE III. The electronic dissociation energy D_e (CCSD(T)-F12/aug-cc-pVQZ[a]), the total change of harmonic vibrational zero-point energy upon complexation ΔZPE (MP2/aug-cc-pVTZ), and the resulting absolute dissociation energy D_0 for the two most stable we_{g+} and we_t conformations of the mixed isotopic ethanol/water complex (units of kJ mol^{-1}).

	we_{g+}	we_{g+}(d1)	we_{g+}(d6)	w(d2)e_{g+}
D_e	26.50	26.50	26.50	26.50
ΔZPE	8.33	8.21	7.96	6.68
D_0	18.17	18.29	18.54	19.82
	we_t	we_t(d1)	we_t(d6)	w(d2)e_t
D_e	25.94	25.94	25.94	25.94
ΔZPE	8.05	7.85	7.64	6.39
D_0	17.89	18.09	18.30	19.55

[a]Electronic dissociation energies D_e calculated at the CCSD(T)-F12/aug-cc-pVQZ level based on optimized geometries at the MP2/aug-cc-pVQZ level.

change of vibrational ZPE upon complexation accounts for between 6.4 and 8.3 kJ mol^{-1} in the harmonic approximation depending on the isotopic substitutions and the hydrogen donor/acceptor roles. In terms of the two most stable we_t and we_{g+} conformations, the benchmark dissociation energy difference prediction $D_e(we_{g+})$–$D_e(we_t)$ of 0.56 kJ mol^{-1} is translated into a smaller 0.28 kJ mol^{-1} difference between the resulting absolute D_0-values. A smaller difference of 0.20 kJ mol^{-1} between the resulting absolute D_0-values for the two most stable conformations of the ethanol-d1/water complex is predicted. These predictions help to explain the fact that both conformations are clearly observed in the far-infrared neon matrix isolation spectra recorded for ethanol-d1/water mixtures.

C. The effects of weak secondary CH···O hydrogen bonding

A closer look at these two normal mode pictures reveals that whereas the out-of-plane donor OH librational mode exhibits an almost localized motion of the bound hydrogen atom almost independent of the dangling OH group on the water molecule, the in-plane mode donor OH librational mode can essentially be pictured as a hindered overall *c*-axis rotation of the water subunit. The latter large-amplitude in-plane OH librational motion of the entire water molecule is therefore expected to be affected more by the weaker secondary O···HC hydrogen bond interaction between the terminal CH group on ethanol and the oxygen lone pair on the water subunit. This has been observed previously for OH librational motion of hydroxy-group containing molecules in crystalline phases.[43,44] In a series of electronic structure calculations at the MP2/aug-cc-pVTZ level, the secondary O···HC hydrogen bond contact of the we_{g+} conformation has been kept as a fixed parameter in the geometry optimizations and subsequent harmonic force field calculations. The predicted harmonic band origins for the intramolecular donor OH-stretching band origin and the two intermolecular donor OH librational band origins versus the displacement R–R_e from the equilibrium value of the intermolecular CH···O hydrogen bond distance are shown in Fig. 5.
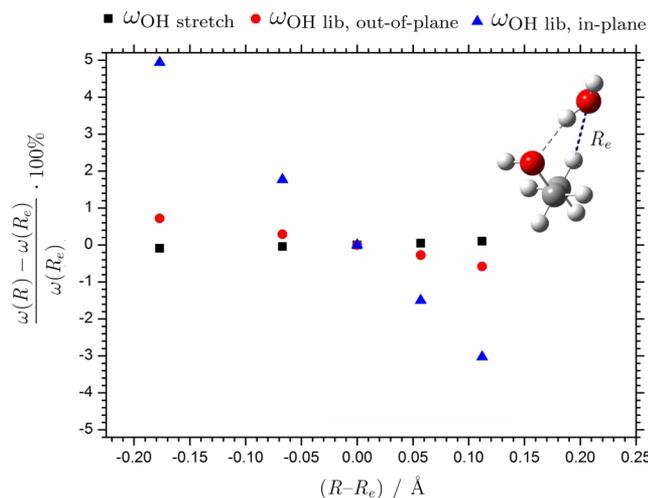
FIG. 5. The predicted relative harmonic band origins (cm^{-1}) of the intramolecular donor OH-stretching mode (black squares) and the high-frequency out-of-plane (red circles) and low-frequency in-plane (blue triangles) donor OH librational modes at the MP2/aug-cc-pVTZ level as a function of the displacement $R-R_e$ (Å) away from the intermolecular equilibrium O···HC hydrogen bond distance for the most stable we_{g+} conformation.

The predicted harmonic band origin of the intramolecular donor OH-stretching mode is lowered by less than 1.5 cm^{-1} when the O···HC hydrogen bond distance is shortened by 0.075 Å relative to the equilibrium configuration. This small predicted red-shift of the intramolecular OH-stretching band origin corresponds to a relative spectral shift of less than 0.05%. This almost non-existent dependence of O···HC contact is expected as this vibrational mode is highly localized into the intramolecular O–H bond of the water subunit involved in the primary OH···O hydrogen bond. The absolute harmonic band origin of the intermolecular large-amplitude out-of-plane donor OH librational mode, on the other hand, is predicted to increase by ca. 2 cm^{-1} when the secondary O···HC hydrogen bond distance is shortened by 0.075 Å. The relative blue-shift for this out-of-plane OH librational mode of 0.4% confirms the nature of a highly localized vibrational mode associated mainly with the primary intermolecular OH···O hydrogen bond. The intermolecular large-amplitude in-plane donor OH librational band origin, however, is predicted to depend much more significantly on the intermolecular O···HC hydrogen bond distance. The harmonic band origin of this hindered overall c-axis rotation of the water subunit is predicted to increase by ca. 7.5 cm^{-1} and thereby relatively blue-shifted by 2.5% when the O···HC interaction is shortened by 0.075 Å. This more significant dependence on the O···HC hydrogen bond distance supports the assumption that the large-amplitude in-plane donor OH librational mode involving the entire water subunit provides an excellent far-infrared spectroscopic probe for the secondary intermolecular hydrogen bond interaction. The proposed assignments of the bands observed at 320.9 cm^{-1} and 314.7 cm^{-1} to the we_{g+}-d1 and we_t-d1 conformations of the ethanol-d1/water complex, respectively, thus seem reasonable in view of the shorter secondary O···HC hydrogen bond distance in the most stable conformation.

VI. CONCLUSIONS

The class of large-amplitude intermolecular donor OH librational modes for the mixed ethanol-water complex has been observed and unambiguously assigned in the challenging far-infrared spectral region enabled by a dual inlet neon matrix deposition approach and explorative electronic structure calculations. These far-infrared spectroscopic observables confirm *directly* electronic structure calculations showing that water acts as the hydrogen bond donor in the two most stable conformations of the mixed complex with ethanol. In the most stable and most compact we_{g+} conformation, electronic structure calculations predict that an intermolecular primary O···HO hydrogen bond is formed between the water subunit and a lone pair of the oxygen atom on the ethanol subunit with a secondary cooperative hydrogen bond interaction between the terminal CH group on ethanol and the oxygen lone pair on water. In this most stable conformation, the water subunit forces the ethanol hydrogen bond partner into its less stable *gauche* conformation upon complexation although the *trans* conformation is the most stable conformation for an isolated ethanol molecule. The second most stable we_t conformation of the mixed complex having water as the hydrogen bond donor and the acceptor ethanol subunit in its *trans* configuration is also further stabilized by a weaker intermolecular O···HC hydrogen bond. Its nature as a localized motion of the "bound" hydrogen atom makes the high-frequency out-of-plane donor OH librational mode an excellent spectroscopic probe for the primary intermolecular O···HO hydrogen bond energy in a similar fashion as the well-known Badger-Bauer relationship associated with the bathochromic shift of the intramolecular donor OH stretching band.[14] The low-frequency in-plane donor OH librational mode of the mixed ethanol/water complex, essentially a hindered overall c-axis rotation of the water subunit, has proven a valuable spectroscopic probe for the secondary intermolecular hydrogen bond interactions as supported by electronic structure calculations. The present findings thus indicate that these large-amplitude donor OH librational motions in general may be helpful for far-infrared spectroscopic detection of conformations for more complex biological systems where the interplay between multiple intermolecular organic hydrogen bond interactions defines the multidimensional conformational potential energy landscapes of the systems.

[1]J. R. Durig and R. A. Larsen, J. Mol. Struct. **238**, 195–222 (1989).
[2]J. C. Pearson, K. V. L. N. Sastry, E. Herbst, and F. de Lucia, J. Mol. Spectrosc. **175**, 246–261 (1996).
[3]E. E. Fileti and S. Canuto, Int. J. Quantum Chem. **104**, 808–815 (2005).
[4]E. E. Fileti, M. A. Castro, and S. Canuto, Chem. Phys. Lett. **452**, 54–58 (2008).

[5]C. Cézard, C. A. Rice, and M. A. Suhm, J. Phys. Chem. A **110**, 9839–9848 (2006).

[6]R. Wugt Larsen, P. Zielke, and M. A. Suhm, J. Chem. Phys. **126**, 194307 (2007).

[7]M. Nedić, T. N. Wassermann, R. Wugt Larsen, and M. A. Suhm, Phys. Chem. Chem. Phys. **13**, 14050–14063 (2011).

[8]M. Nedić, T. N. Wassermann, Z. Xue, P. Zielke, and M. A. Suhm, Phys. Chem. Chem. Phys. **10**, 5953–5956 (2008).

[9]I. A. Finneran, P. B. Carroll, M. A. Allodi, and G. A. Blake, Phys. Chem. Chem. Phys. **17**, 24210–24214 (2015).

[10]R. Wugt Larsen and M. A. Suhm, J. Chem. Phys. **125**, 154314 (2006).

[11]R. Wugt Larsen and M. A. Suhm, Phys. Chem. Chem. Phys. **12**, 8152–8157 (2010).

[12]F. Kollipost, J. Andersen, D. W. Mahler, J. Heimdal, M. Heger, M. A. Suhm, and R. Wugt Larsen, J. Chem. Phys. **141**, 174314 (2014).

[13]J. Ceponkus, P. Uvdal, and B. Nelander, J. Chem. Phys. **129**(19), 194306 (2008).

[14]S. H. Bauer and R. M. Badger, J. Chem. Phys. **5**, 837 (1937).

[15]J. Andersen, J. Heimdal, D. W. Mahler, B. Nelander, and R. Wugt Larsen, J. Chem. Phys. **140**, 091103 (2014).

[16]J. Ceponkus and B. Nelander, J. Phys. Chem. A **108**(31), 6499–6502 (2004).

[17]J. Ceponkus, G. Karlstrom, and B. Nelander, J. Phys. Chem. A **109**, 7859–7864 (2005).

[18]J. Ceponkus, P. Uvdal, and B. Nelander, J. Chem. Phys. **133**(7), 074301 (2010).

[19]J. Ceponkus, P. Uvdal, and B. Nelander, J. Phys. Chem. A **114**(25), 6829–6831 (2010).

[20]A. J. Barnes and H. E. Hallam, Trans. Faraday Soc. **66**, 1932–1940 (1970).

[21]J. R. Durig, W. E. Bucy, C. J. Wurrey, and L. A. Carreira, J. Phys. Chem. **79**, 988–993 (1975).

[22]J. C. Pearson, C. S. Brauer, and B. J. Drouin, J. Mol. Spectrosc. **251**, 394–409 (2008).

[23]T. N. Wassermann and M. A. Suhm, J. Phys. Chem. A **114**, 8223–8233 (2010).

[24]M. L. Senent, Y. G. Smeyers, R. Dominguez Gomez, and M. Villa, J. Chem. Phys. **112**, 5809–5819 (2000).

[25]J. Andersen, J. Heimdal, and R. Wugt Larsen, Phys. Chem. Chem. Phys. **17**, 23761–23769 (2015).

[26]N. Bakkas, Y. Bouteiller, A. Loutellier, J. P. Perchard, and S. Racine, J. Chem. Phys. **99**, 3335–3342 (1993).

[27]N. Bakkas, Y. Bouteiller, A. Loutellier, J. P. Perchard, and S. Racine, Chem. Phys. Lett. **232**, 90–98 (1995).

[28]S. Coussan, P. Roubin, and J. P. Perchard, J. Phys. Chem. A **108**, 7331–7338 (2004).

[29]M. J. Frisch, G. W. Trucks, H. B. Schlegel, G. E. Scuseria, M. A. Robb, J. R. Cheeseman, G. Scalmani, V. Barone, B. Mennucci, G. A. Petersson, H. Nakatsuji, M. Caricato, X. Li, H. P. Hratchian, A. F. Izmaylov, J. Bloino, G. Zheng, J. L. Sonnenberg, M. Hada, M. Ehara, K. Toyota, R. Fukuda, J. Hasegawa, M. Ishida, T. Nakajima, Y. Honda, O. Kitao, H. Nakai, T. Vreven, J. A. Montgomery, Jr., J. E. Peralta, F. Ogliaro, M. Bearpark, J. J. Heyd, E. Brothers, K. N. Kudin, V. N. Staroverov, R. Kobayashi, J. Normand, K. Raghavachari, A. Rendell, J. C. Burant, S. S. Iyengar, J. Tomasi, M. Cossi, N. Rega, J. M. Millam, M. Klene, J. E. Knox, J. B. Cross, V. Bakken, C. Adamo, J. Jaramillo, R. Gomperts, R. E. Stratmann, O. Yazyev, A. J. Austin, R. Cammi, C. Pomelli, J. W. Ochterski, R. L. Martin, K. Morokuma, V. G. Zakrzewski, G. A. Voth, P. Salvador, J. J. Dannenberg, S. Dapprich, A. D. Daniels, O. Farkas, J. B. Foresman, J. V. Ortiz, J. Cioslowski, and D. J. Fox, GAUSSIAN 09, Revision D.01, Gaussian, Inc., Wallingford, CT, 2009.

[30]R. Ahlrichs, M. Baer, M. Haeser, H. Horn, and C. Koelmel, Chem. Phys. Lett. **162**, 165–169 (1989).

[31]F. Furche, R. Ahlrichs, C. Haettig, W. Klopper, M. Sierka, and F. Weigend, WIREs: Comput. Mol. Sci. **4**, 91–100 (2014).

[32]A. D. Becke, J. Chem. Phys. **98**, 5648–5652 (1993).

[33]S. E. S. Grimme, J. Antony, and H. Krieg, J. Chem. Phys. **132**, 154104 (2010).

[34]C. Møller and M. Plesset, Phys. Rev. **46**, 618 (1934).

[35]K. Raghavachari and J. A. Pople, Int. J. Quantum Chem. **14**, 91 (1978).

[36]R. A. Kendall, J. T. H. Dunning, and R. J. Harrison, J. Chem. Phys. **96**, 6796–6806 (1992).

[37]J. A. Pople, M. Head-Gordon, and K. Raghavachari, J. Chem. Phys. **87**, 5968 (1987).

[38]T. B. Adler and H.-J. Werner, J. Chem. Phys. **135**, 144117 (2011).

[39]B. J. Ransil, J. Chem. Phys. **34**, 2109 (1961).

[40]S. F. Boys and F. Bernardi, Mol. Phys. **19**, 553–566 (1970).

[41]V. Barone, J. Chem. Phys. **122**, 14108 (2005).

[42]A. Sharma, I. Reva, R. Fausto, S. Hesse, M. A. Suhm, S. K. Nayak, R. Sathiskumar, R. Pal, and T. N. G. Row, J. Am. Chem. Soc. **133**, 20194 (2011).

[43]S. Jarmelo, I. Reva, M. Rozenberg, M. Ramos Silva, A. M. Matos Beja, and R. Fausto, J. Phys. Chem. B **112**, 8032–8041 (2008).

[44]See supplementary material at http://dx.doi.org/10.1063/1.4937482 for the calculated absolute electronic energies employing the B3LYP, B3LYP-D3, MP2, CCSD(T), and CCSD(T)-F12 methodologies with the aug-cc-pVTZ and aug-cc-pVQZ basis sets and the calculated harmonic vibrational zero-point energy corrections employing the MP2/aug-cc-pVTZ method.